Supporting Information

Synthesis of Mo and Ru solid-solution alloy NPs via thermal decomposition and their hydrogen evolution reaction activity

Shinya Okazoe[a], Kohei Kusada[a], Dongshuang Wu[a], Tomokazu Yamamoto[b,c], Takaaki Toriyama[c], Syo Matsumura[b,c], Shogo Kawaguchi[d], Yoshiki Kubota[e] and Hiroshi Kitagawa [a]

a. *Division of Chemistry, Graduate School of Science, Kyoto University, Kitashirakawa-Oiwakecho, Sakyo-ku, Kyoto 606-8502, Japan.*

b. *Department of Applied Quantum Physics and Nuclear Engineering, Kyushu University, 744 Motooka, Nishi-ku, Fukuoka 819-0395, Japan.*

c. *The Ultramicroscopy Research Center, Kyushu University, Motooka 744, Nishi-ku, Fukuoka 819-0395, Japan.*

d. *Japan Synchrotron Radiation Research Insitute (JASRI), SPring-8, 1-1-1 Kouto, Sayo-cho, Sayo-gun, Hyogo 679-5198, Japan*

e. *Department of Physical Science, Graduate School of Science, Osaka Prefecture University, Sakai, Osaka 599-8531, Japan.*

Materials

Molybdenum hexacarbonyl ($Mo(CO)_6$) and triruthenium dodecacarbonyl ($Ru_3(CO)_{12}$) were purchased from Sigma-Aldrich (USA). $RuCl_3 \cdot nH_2O$, poly(N-vinyl-2-pyrrolidone) (PVP, K30, molecular weight, Mw≈40,000), ethylene glycol (EG), hexane, acetone, ethanol, diethyl ether, tetrahydrofuran (THF), isopropanol, potassium hydroxide (KOH), sulfuric acid (H_2SO_4), and 5 wt% Nafion solution were purchased from Wako (Japan). Twenty wt% Pt NPs on carbon black powder were purchased from Alfa Aesar (USA). Oleylamine (OAm) was purchased from Acros Organics (USA). Doubly distilled deionized water (18.2 MΩ) produced by Direct-Q UV (Merck, USA) was used for all experiments.

Synthesis of Mo–Ru solid-solution alloy NPs

To synthesize the Mo–Ru solid-solution alloy NPs, we chose $Mo(CO)_6$ and $Ru_3(CO)_{12}$ as precursors. OAm was chosen as solvent and protective agent. OAm was evacuated under 2 kPa at 100 °C for 1 h to remove residual water. After purging nitrogen gas, $Mo(CO)_6$ (1.9 mmol) and $Ru_3(CO)_{12}$ (1.9 mmol) were added to OAm (120 mL), and the solution was heated in a three-neck flask in a heating mantle at 330 °C for 2 h. After the reaction was complete, the product was separated by centrifugation with hexane and acetone.

Synthesis of Ru NPs by a liquid phase reduction method[1]

To synthesize hexagonal close-packed (hcp) structure Ru NPs, $RuCl_3 \cdot nH_2O$ (1.0 mmol, Wako) and PVP (2.5 mmol of monomer units, Wako) were dissolved in EG (25 mL, Wako) at room temperature. The solution was then heated to 200 °C and maintained at this temperature for 3 h. After the reaction was complete, the product was separated by centrifugation with ethanol, diethyl ether, and acetone.

Synthesis of Ru NPs by a thermal decomposition

To prepare the Ru NPs by a thermal decomposition, OAm was evacuated under 2 kPa at 100 °C for 1 h to remove residual water. After purging nitrogen gas, $Ru_3(CO)_{12}$ (xx mmol) were added to OAm (120 mL), and the solution was heated in a three-neck flask in a heating mantle at 330 °C for 2 h. After the reaction was complete, the product was separated by centrifugation with hexane and acetone.

Characterization

The structure of the NPs was determined by synchrotron PXRD measurement (λ = 0.62921 Å, scan step: 0.006°) at SPring-8 beamline BL02B2 and D8 ADVANCE (Bruker) as a lab PXRD. Rietveld refinement of the PXRD pattern was performed using TOPAS3 (Bruker

AXS). The size of NPs was determined by HT7700 (Hitachi) transmission electron microscopy (TEM) operated at 100 kV. The atomic ratios of Mo and Ru in the NPs or the catalyst were determined by ZSX Primus IV (Rigaku) XRF instrument. High-angle annular dark-field (HAADF)-STEM observation and STEM-energy dispersive X-ray spectroscopy (EDX) mapping and line analysis were performed using an aberration-corrected electron microscope JEOL JEM-ARM 200F operated at 120 kV at The Ultramicroscopy Research Center, Kyushu University. X-ray photoelectron spectroscopy (XPS) spectra were obtained by ESCA-3400 (Shimadzu) X-ray photoelectron spectrometer. The surface of bulk Mo and Ru powder samples were etched by Ar ions to remove oxidized surface and obtain metallic surface. Obtained XPS spectra were analyzed by XPSfit41 software. The binding energies were corrected with reference to the C(1s) line at 284.6 eV.

Catalyst preparation

MoRu solid-solution alloy NPs (5 mg) in metal dispersed in 35 mL of THF were sonicated for 3 h and mixed with 40 mg of Vulcan XC 72R carbon dispersed into 7.5 mL of isopropanol. After sonicating for 4 h, the product was centrifuged and dried. Next, the product was added to 50 mL acetic acid and stirred at 60 °C for 16 h. The catalyst (5 mg) was suspended and sonicated in 1.9 mL isopropanol and 0.1 mL Nafion solution. The catalyst ink (10 μL) was deposited on a 5 mm diameter glassy carbon working electrode (BAS). The effect of acetic acid wash on the HER catalytic activities of MoRu/C was investigated. As shown in Fig. S17, MoRu/C catalyst after the wash showed larger current densities in CV and polarization curve, which suggested that much electrocatalytically active sites were exposed by the washing process.

Ru NP synthesized by a liquid phase reduction catalyst was prepared with the same procedure using 35 mL deionized water as a solvent.

Electrochemical measurements

All electrochemical tests were performed using a CHI 760eE electrochemical workstation (CHI instruments, Inc., USA) connected with a RRDE-3A constant rotation system (ALS Co., Ltd, Japan). We used a conventional three-electrode system: a Hg/HgO reference electrode (1.0 M KOH), a glassy carbon electrode (3 mm diameter, 10 cm in length), and an RDE (5 mm disk diameter) as a working electrode. The reference electrode was calibrated at room temperature before each test, and all potentials are reported relative to the RHE. All of the catalysts had the same metal mass weight and were loaded onto a glassy carbon RDE. Each catalyst was swept from 0.04 to 0.94 V at a sweep rate of 200 mV s^{-1} for dozens of cycles in

an Ar-saturated 1.0 M KOH solution to obtain a stable and clean electrode surface before the HER tests. After the electrochemical cleaning, cyclic voltammetry (Fig. S15) was measured at a sweep rate of 20 mV s^{-1}.

To determine the HER activity, linear sweep voltammetry (LSV) was measured at a sweep rate of 5 mV s^{-1} at 1600 rpm in an Ar-saturated 1.0 M KOH solution. All polarization curves were corrected with 80% *iR* compensation in the solution after each scan. All of the electrochemical measurements were repeated at least three times to confirm reproducibility.To determine the electrochemical active surface area (ECSA), a Cu underpotential deposition method was used.[2] Each catalyst was first swept from 0.04 to 0.94 V at a sweep rate of 500 mV s^{-1} for dozens of cycles in an Ar-saturated 1.0 M KOH solution to obtain a stable and clean electrode surface before the ECSA tests. Then, the electrodes were fixed at a certain deposition potential for 100 s in the electrolyte of 5 mM $CuSO_4$/0.5 M H_2SO_4 and followed by a CV scan from the fixed to the higher potential. The charges associated with Cu stripping were obtained by using the charge associated with any oxide growth and subtracting the charge obtained under the same conditions in 0.5 M H_2SO_4. A specific charge of 0.42 mC cm^{-2} was used to convert the coulombic charge to the surface area. To evaluate stability of the catalyst, chronoamperometry was performed for 2 hours. The catalyst was applied the specific voltage that achieves 10 mA cm^{-2} referring to the polarization curve.

Table S1 The parameters of Rietveld refinement of the synchrotron PXRD pattern for the hcp component of MoRu solid-solution alloy NPs.

Atom	*x*	*y*	*z*	*B* / Å^2	Occ.	Lattice constat /Å	
						a_{hcp}	c_{hcp}
Mo	1/3	2/3	1/4	0.5015	0.15	2.7882(7)	4.3716(9)
Ru	1/3	2/3	1/4	0.5003	0.85		

Table S2 The parameters of Rietveld refinement of the synchrotron PXRD pattern for the fcc component of MoRu solid-solution alloy NPs.

Atom	*x*	*y*	*z*	*B* / Å^2	Occ.	Lattice constat / Å
						a_{fcc}
Mo	0	0	0	0.5002	0.15	3.8560(7)
Ru	0	0	0	0.5002	0.85	

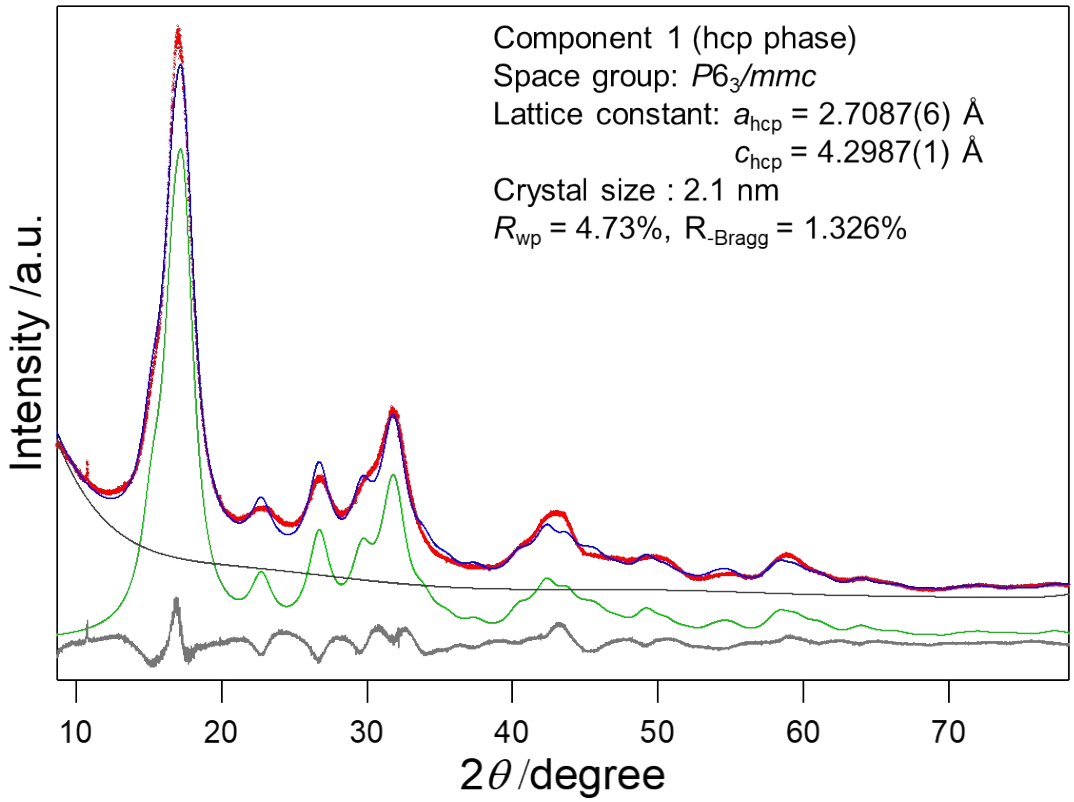

Fig. S1 Synchrotron XRD analysis of Ru NPs at room temperature, 2 θ = 8.70 to 78.21 degrees. The radiation wavelength was 0.62921 Å. The diffraction pattern is shown as red dots. The calculated pattern is shown as the blue line. The difference profile, and the background and fitting curves of hcp component are shown as grey, black, and green lines, respectively.

Table S3 The parameters of Rietveld refinement of the synchrotron PXRD pattern for the hcp component of Ru NPs.

Atom	*x*	*y*	*z*	*B* / Å^2	Occ.	Lattice constat / Å	
						a	*c*
Ru	1/3	2/3	1/4	0.500(11)	1	2.7087(6)	4.2987(1)

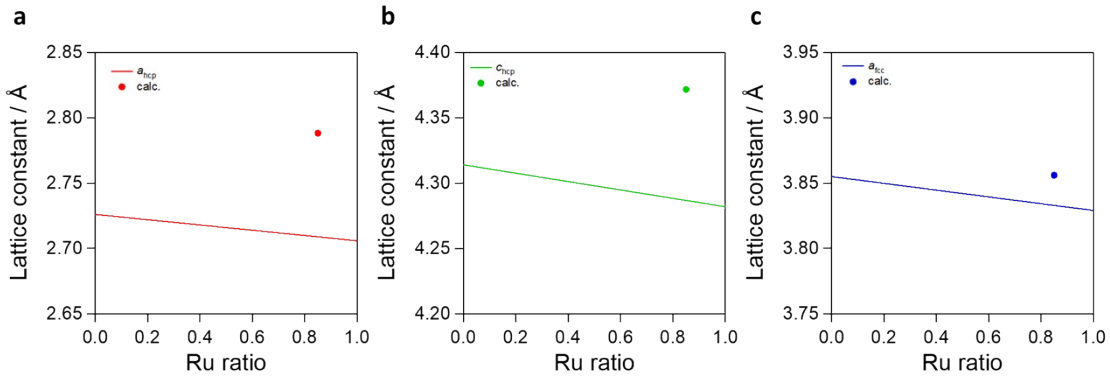

Fig. S2 Comparison of lattice constants for **a** a_{hcp} **b** c_{hcp} and **c** a_{fcc}. The lines indicate the ideal lattice constants estimated from Vegard's law, and the circles are calculated values by Rietveld refinement.

The lattice constants *a* and *c* of hcp Ru are 2.7059 and 4.2819 Å, respectively (PDF #00-006-0663). The ratio *c*/*a* is the factor that determines the lattice, and it depends on the metals. In the case of bulk Ru, *c*/*a* is 1.5824; we used this value for the c_{hcp} calculation of Mo. The atomic radius (*r*) and lattice constants (*a*) of bcc, fcc, and hcp structures are calculated theoretically,

$$4r = \sqrt{3}\, a_{bcc}$$

$$4r = \sqrt{2}\, a_{fcc}$$

$$2r = a_{hcp}$$

Using these equations, the lattice constants of Mo were calculated. The atomic radius of Mo calculated from the bcc structure (a=3.147 Å, PDF #00-004-0809) was 1.363 Å. Therefore, the values of a_{hcp}, c_{hcp}, and a_{fcc} are 2.726, 4.314, and 3.855 Å, respectively. For fcc Ru, we used the reported value (PDF #01-088-2333).

In general, the lattice constants of solid-solution alloys follow Vegard's law. However, the lattice constants of the Mo–Ru solid-solution alloy NPs are larger than expected. This result implies that carbon exists in lattice voids.

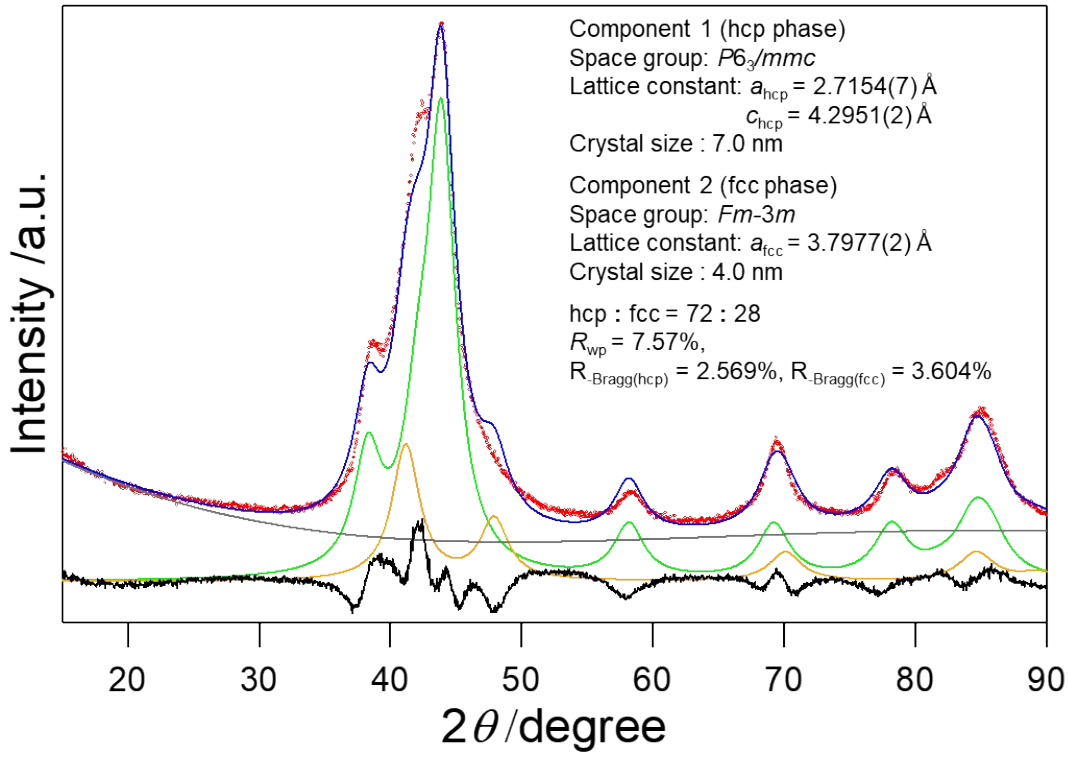

Fig. S3 XRD analysis of Ru NPs synthesized by the thermal decomposition at room temperature, 2 θ = 15 to 90 degrees. The radiation wavelength was 1.5418 Å (Cu-$K\alpha$). The diffraction pattern is shown as red dots. The calculated pattern is shown as the blue line. The difference profile, and the background and fitting curves of hcp and fcc components are shown as grey, black, green, and yellow lines, respectively.

Table S4 The parameters of Rietveld refinement of the PXRD pattern for the hcp component of Ru NPs synthesized by thermal decomposition.

Atom	x	y	z	B / Å^2	Occ.	Lattice constat / A	
						a	c
Ru	1/3	2/3	1/4	0.599(11)	1	2.7087(6)	4.2987(1)

Table S5 The parameters of Rietveld refinement of the PXRD pattern for the fcc component of Ru NPs synthesized by thermal decomposition.

Atom	x	y	z	B / Å^2	Occ.	Lattice constat / A
						a
Ru	0	0	0	0.510(11)	1	3.7967(2)

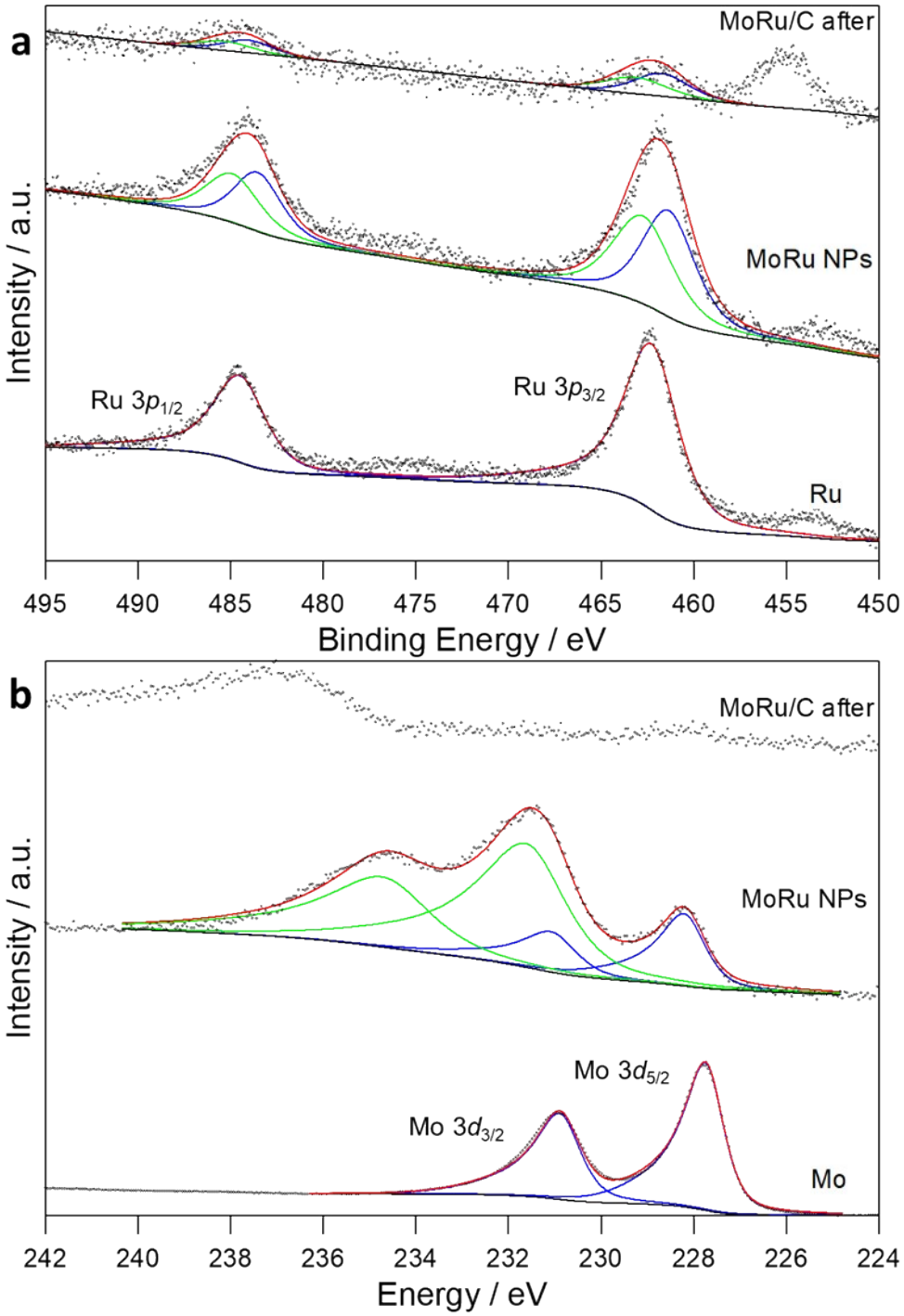

Figure S4 **a** Ru 3*p* and **b** Mo 3*d* XPS spectra of MoRu NPs and MoRu/C after stability test. Those of bulk metals are also shown for a comparison. The observed spectra, sum of fitting peaks, and backgrounds are shown as gray dots, red, and black solid line, respectively. The fitting components of metallic and oxide are shown as blue and green line, respectively.

Table S6 Fitting parameters of Ru 3*p* spectra.

Sample	Peak	Position /eV	FWHM / eV	State	Ratio / %
MoRu/C after stability test	Ru $3p_{3/2}$	461.76	3.42	Metal	55
	Ru $3p_{1/2}$	484.06	3.07		
	Ru $3p_{3/2}$	463.16	3.85	Oxide	45
	Ru $3p_{1/2}$	485.35	3.43		
MoRu NPs	Ru $3p_{3/2}$	461.34	3.38	Metal	52
	Ru $3p_{1/2}$	483.54	3.04		
	Ru $3p_{3/2}$	462.74	3.83	Oxide	48
	Ru $3p_{1/2}$	484.91	3.45		
Ru	Ru $3p_{3/2}$	462.27	3.37	Metal	100
	Ru $3p_{1/2}$	484.49	3.22		

Table S7 Fitting parameters of Mo 3*d* spectra.

Sample	Peak	Position /eV	FWHM / eV	State	Ratio / %
MoRu NPs	Mo $3d_{5/2}$	228.21	1.06	Metal	24
	Mo $3d_{3/2}$	231.08	1.27		
	Mo $3d_{5/2}$	231.63	2.02	Oxide	76
	Mo $3d_{3/2}$	234.73	2.37		
Mo	Mo $3d_{5/2}$	227.75	0.92	Metal	100
	Mo $3d_{3/2}$	230.90	1.05		

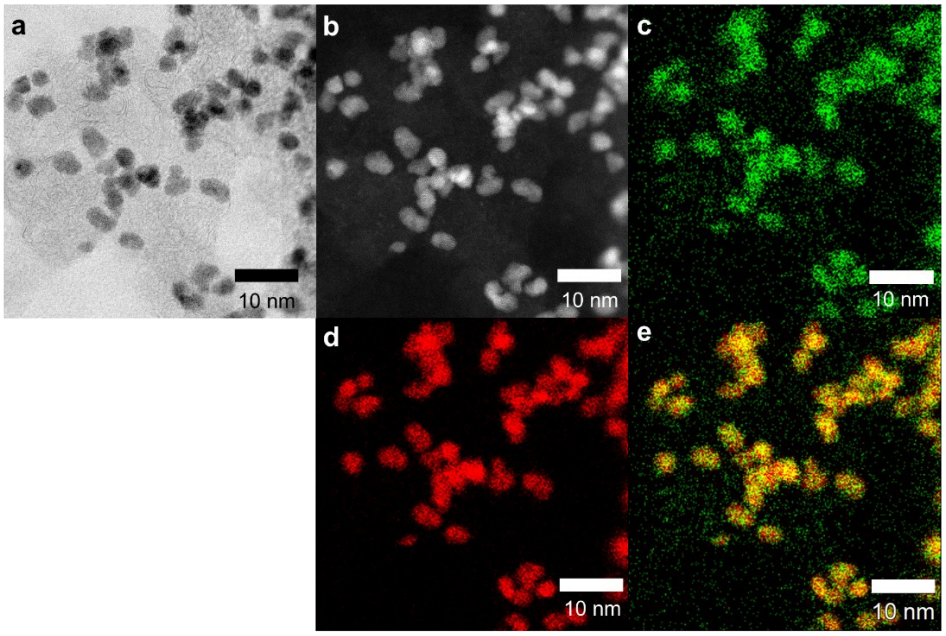

Fig. S5 EDX maps of the synthesized MoRu solid-solution alloy NPs on carbon. **a, b** BF- and HAADF-STEM images of MoRu NPs. **c, d** Mo-*L* and Ru-*L* STEM−EDX maps. **e** Overlay image of **(c)** and **(d)**.

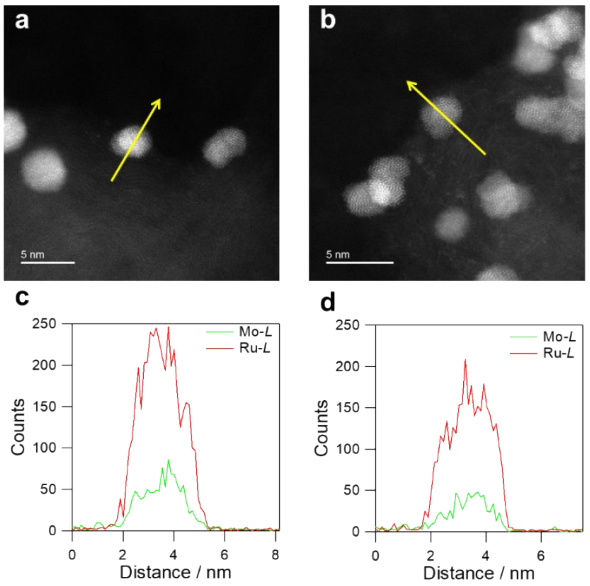

Fig. S6 EDX line profiles of the synthesized MoRu solid-solution alloy NPs on carbon. **a, b** HAADF-STEM image of MoRu NPs. **c, d** EDX line profiles of the MoRu NP along the arrow shown in **(a)**, **(b)** respectively. Mo-*L* and Ru-*L* lines are indicated as green and red lines, respectively.

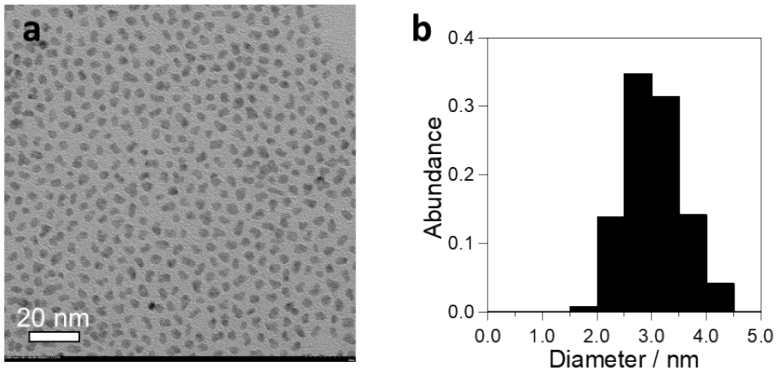

Fig. S7 **a** TEM image of MoRu solid-solution alloy NPs. **b** Histogram of the size of NPs.

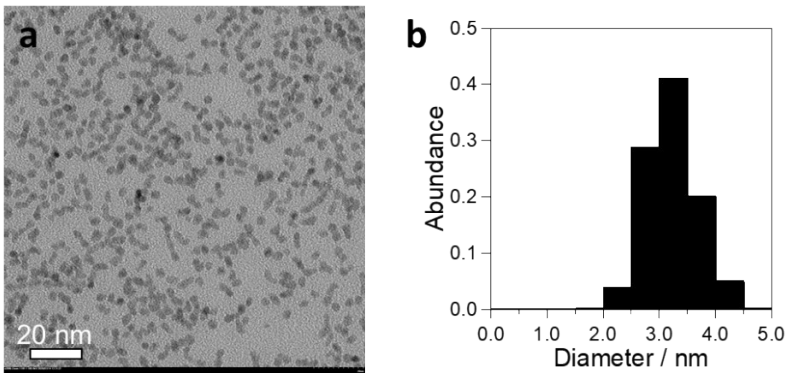

Fig. S8 **a** TEM image of Ru NPs synthesized by a liquid phase reduction. **b** Histogram of the size of NPs.

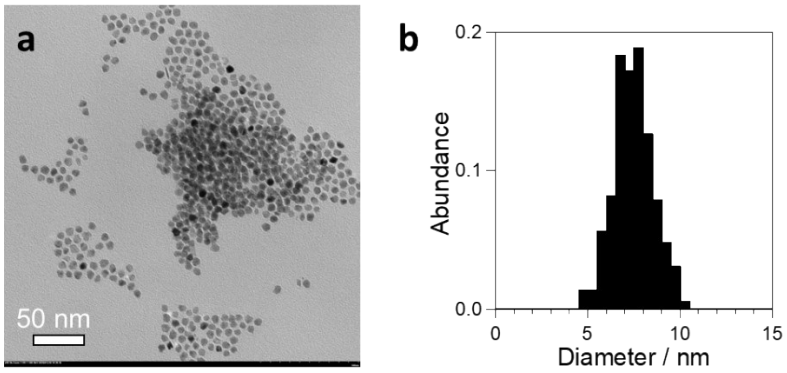

Fig. S9 **a** TEM image of Ru NPs synthesized by the thermal decomposition. **b** Histogram of the size of NPs.

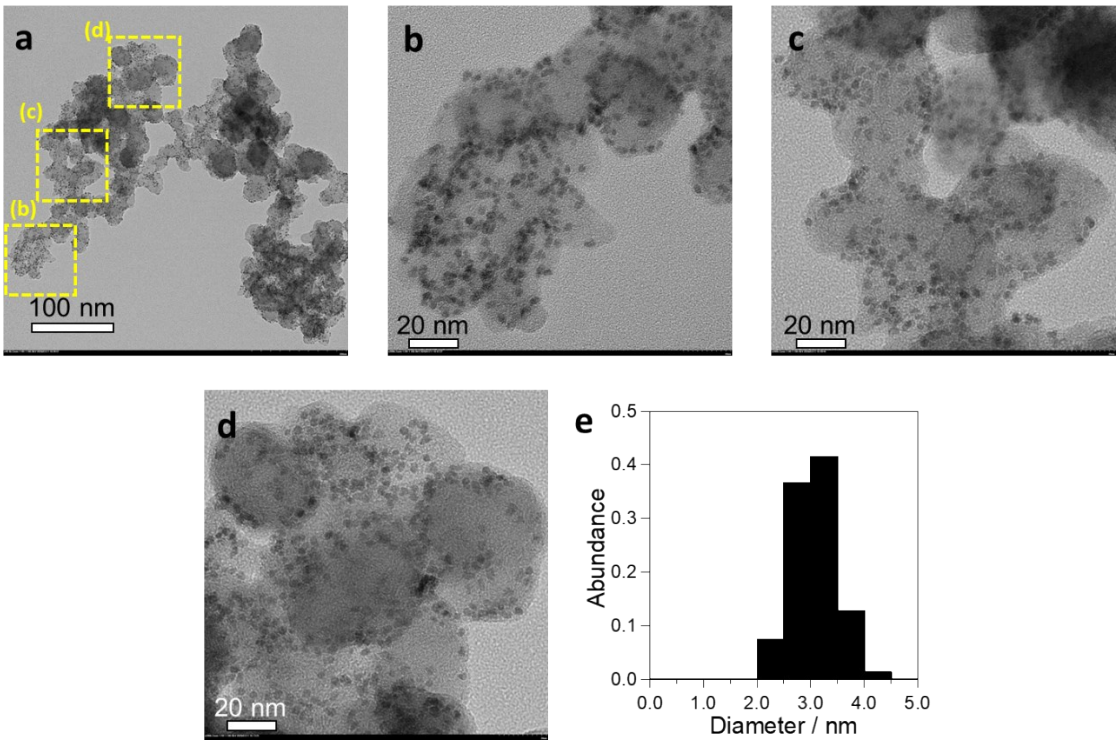

Fig. S10 TEM images of MoRu alloy NPs on carbon after acetic acid washing. **a** Low magnification image. **b, c, d** Expanded images of **(a). e** Histogram of the size of NPs.

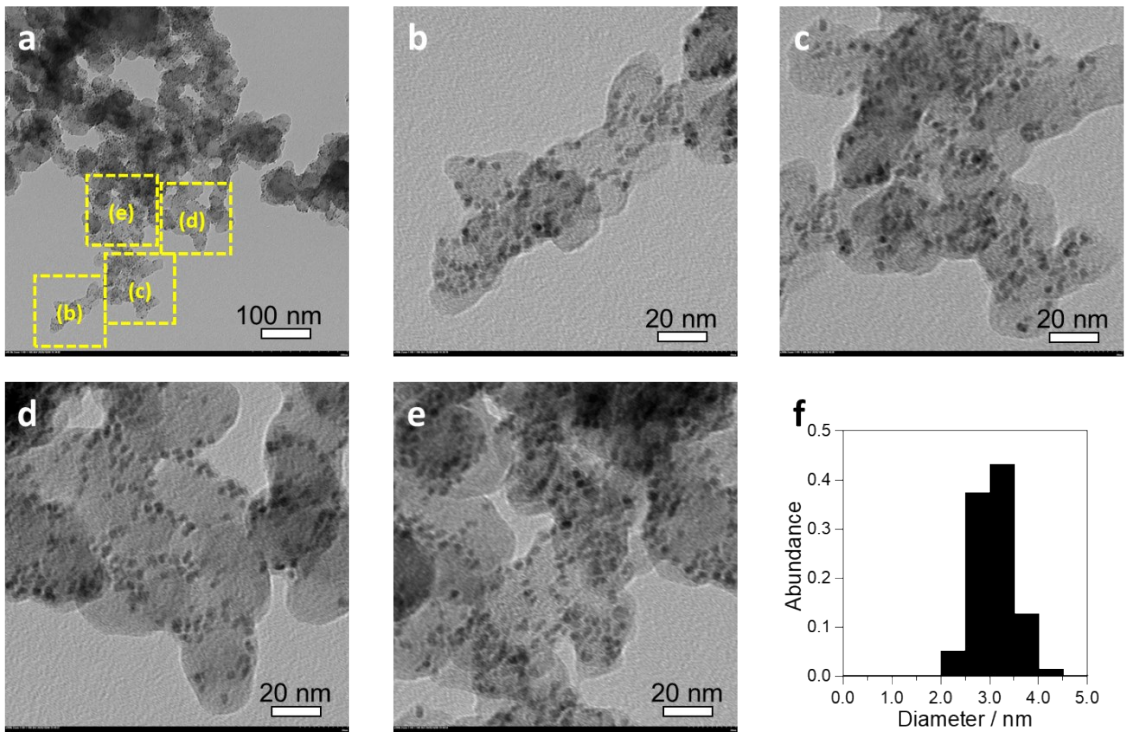

Fig. S11 TEM images of MoRu alloy NPs on carbon before acetic acid washing. **a** Low magnification image. **b, c, d, e** Expanded images of **(a). e** Histogram of the size of NPs.

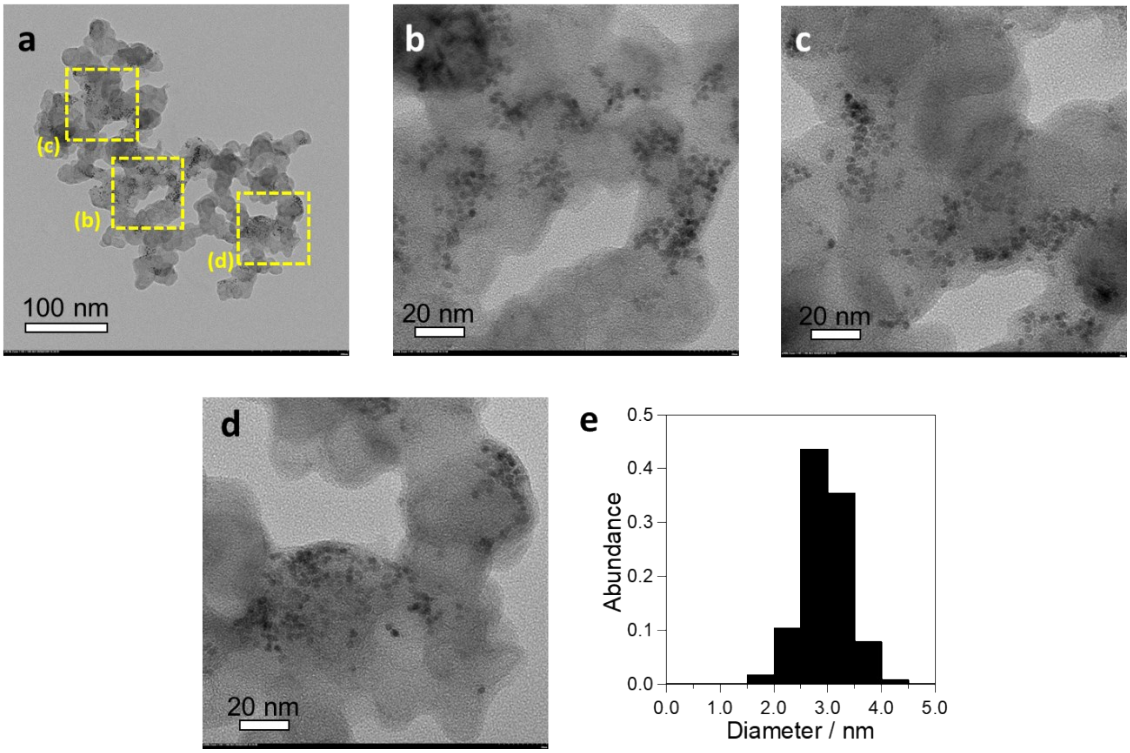

Fig. S12 TEM images of Ru NPs synthesized by the liquid phase reduction on carbon after acetic acid washing. **a** Low magnification image. **b, c, d** Expanded images of **(a). e** Histogram of the size of NPs.

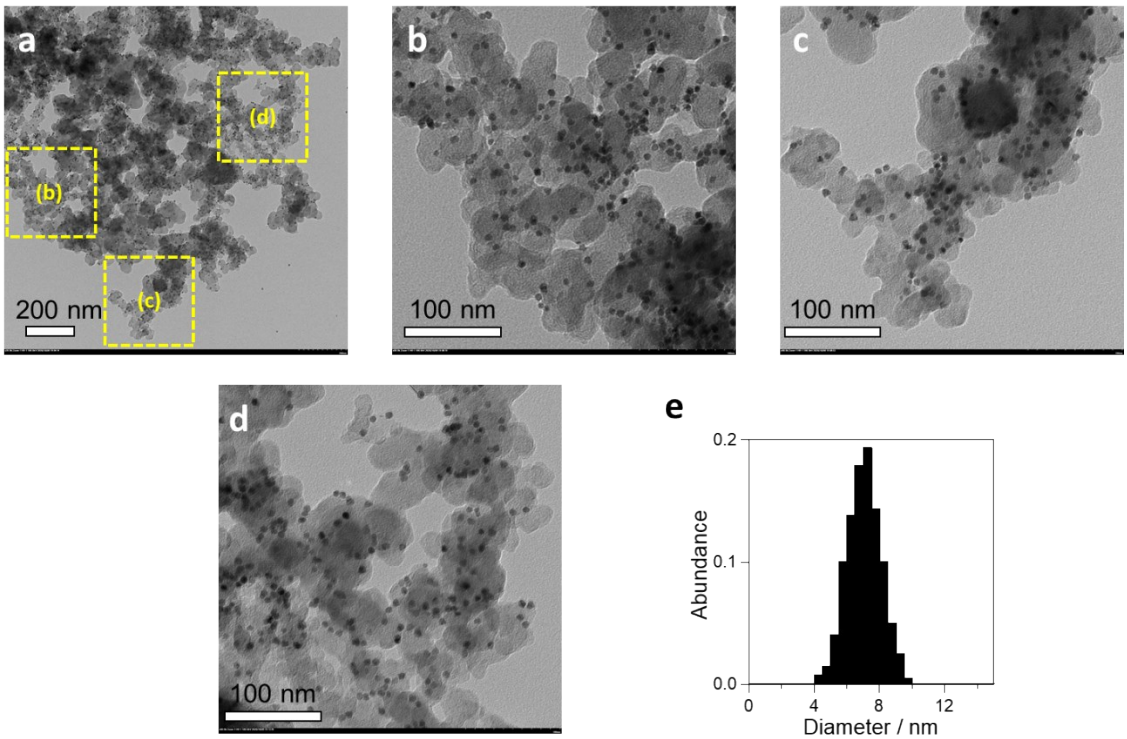

Fig. S13 TEM images of Ru NPs synthesized by the thermal decomposition on carbon after acetic acid washing. **a** Low magnification image. **b, c, d** Expanded images of **(a). f** Histogram of the size of NPs.

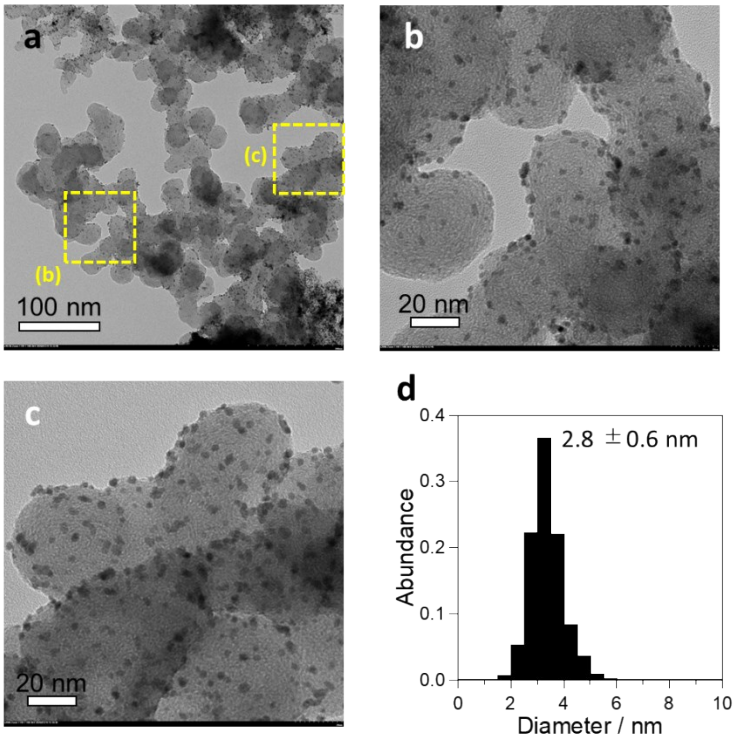

Fig. S14 TEM images of Pt NPs on carbon (commercial). **a** Low magnification image. **b, c** Expanded images of **(a). d** Histogram of the size of NPs.

TableS8 Mean diameter and standard distribution of the samples. 1. Synthesized by liquid phase reduction (L.P.R.). 2. Synthesized by thermal decomposition (T.D.).

Sample	Mean diameter / nm	Standard deviation / nm
MoRu	2.5	0.5
Ru (L.P.R.)[1]	2.7	0.5
Ru (T.D.)[2]	7.0	1.1
MoRu/C (After acetic acid wash)	2.6	0.4
MoRu/C (Before acetic acid wash)	2.6	0.4
Ru/C (L.P.R) (After acetic acid wash)	2.5	0.5
Ru/C (T.D.) (After acetic acid wash)	6.5	1.0
Pt/C	2.8	0.6

The sizes of MoRu and Ru NPs did not change after loading operation onto carbon and acetic acid wash.

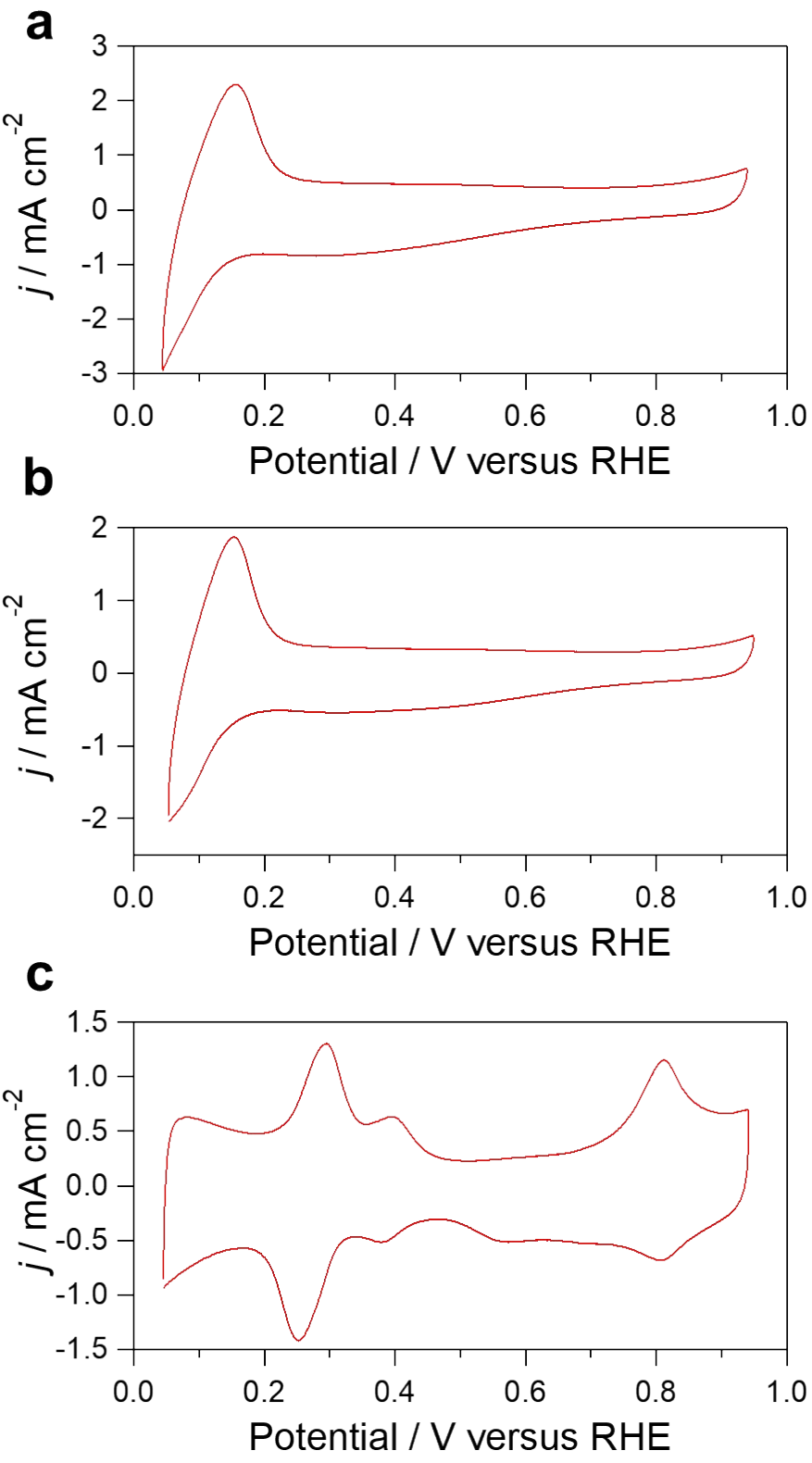

Fig. S15 Cyclic voltammograms of **a** MoRu/C, **b** Ru/C, and **c** Pt/C catalysts, respectively. The scan rate was 20 mV s^{-1}.

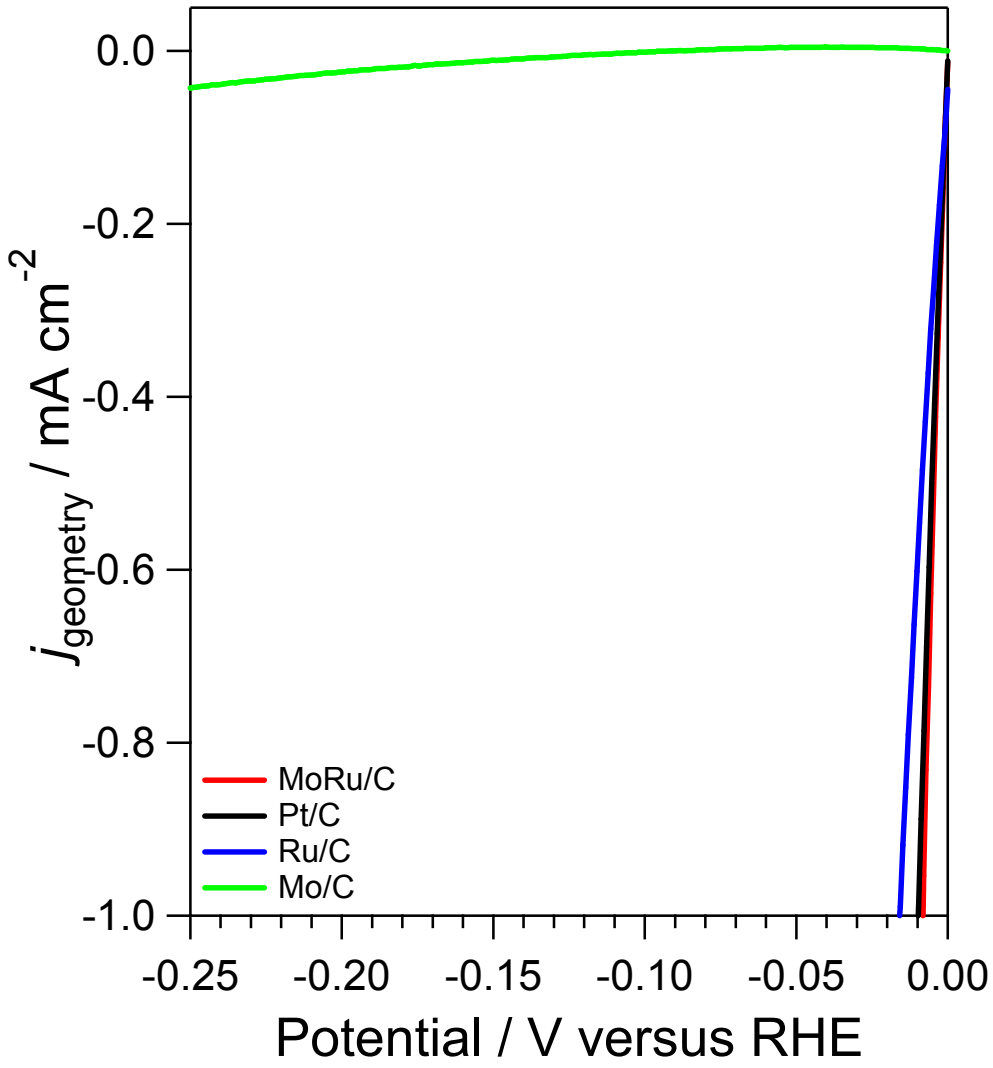

Fig. S16 Polarization curves of 20 wt% Mo/C in 1.0 M KOH solution. Polarization curves of 20 wt% MoRu/C, Pt/C, and Ru/C are shown for a comparison.

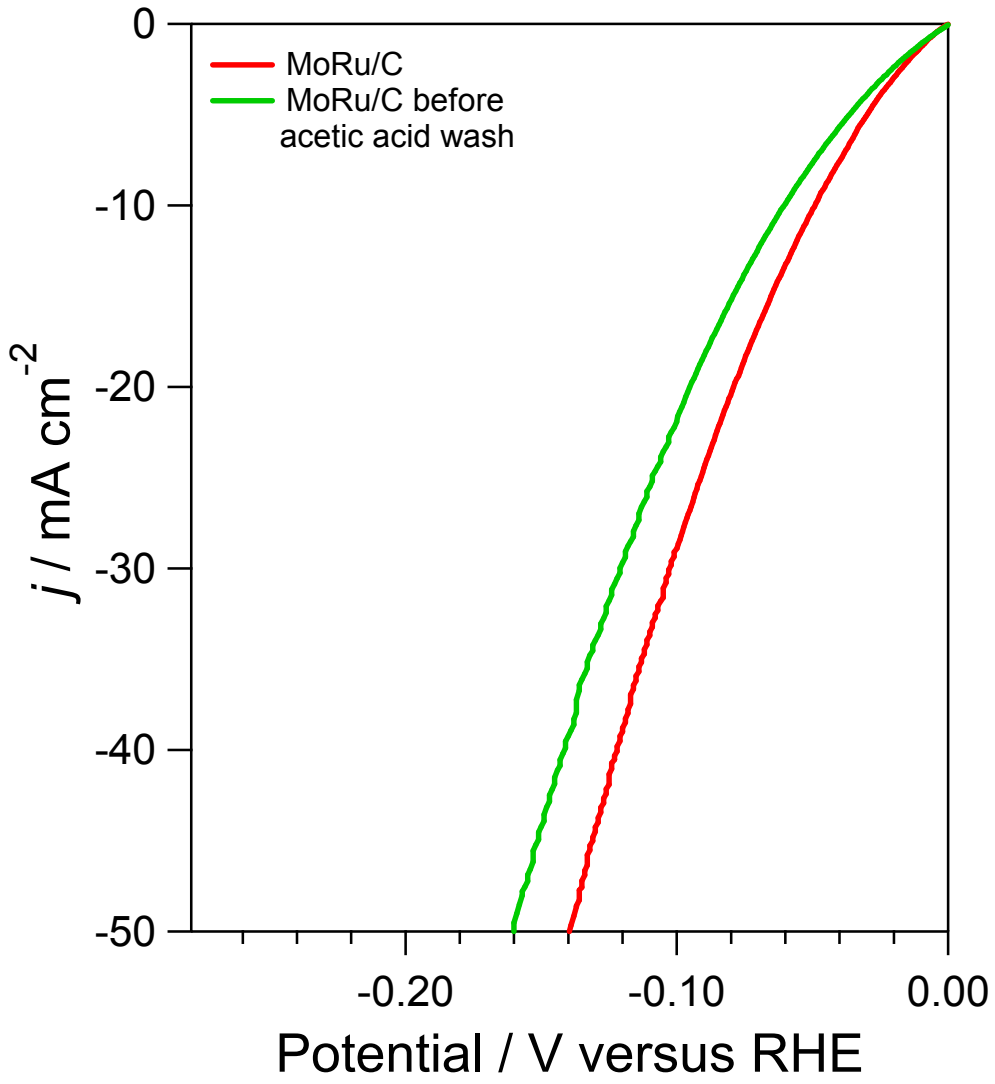

Fig. S17 Polarization curves of 20 wt% MoRu/C before acetic acid washing in 1.0 M KOH solution.

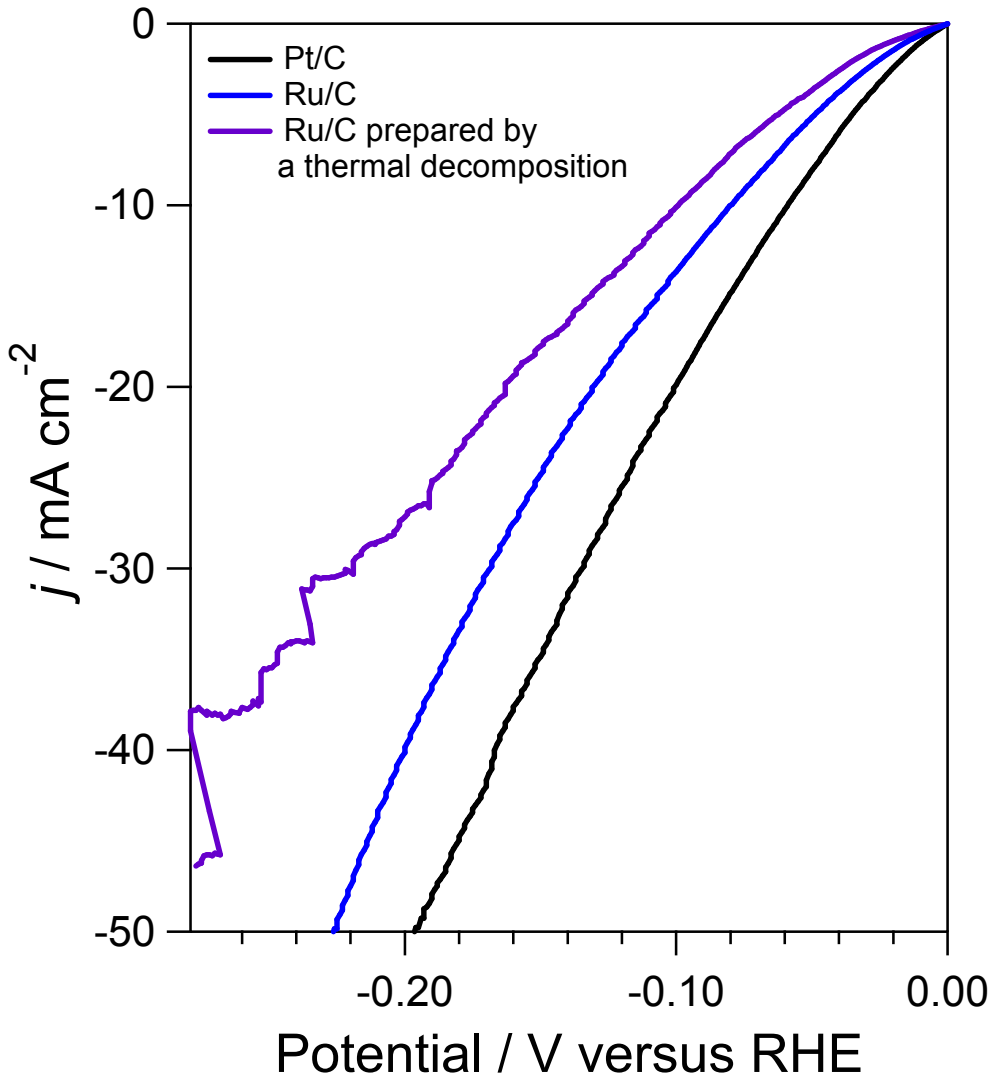

Fig. S18 Polarization curves of 20 wt% Ru/C synthesized by the thermal decomposition in 1.0 M KOH solution. The catalyst was washed with acetic acid. Polarization curves of 20 wt% Pt/C, and Ru/C are shown for a comparison.

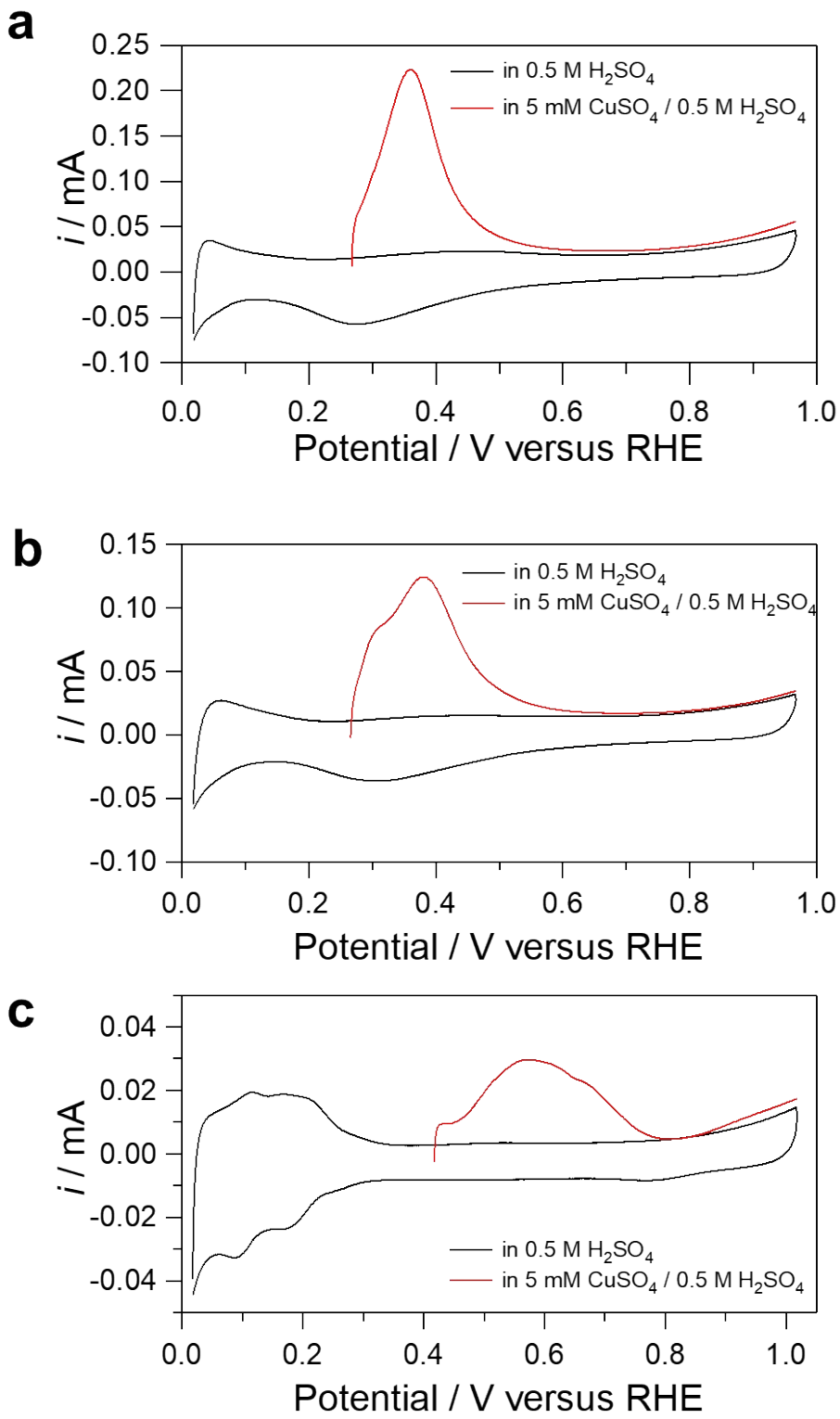

Fig. S19 LSV curves in 5 mM $CuSO_4$/0.5M H_2SO_4 (red) and CV curves in 0.5 M H_2SO_4 (black) of **a** MoRu/C, **b** Ru/C, and **c** Pt/C, respectively.

Table S9 ECSA of catalysts.

catalyst	Electrochemical active surface area / $m^2\ g^{-1}$
MoRu NPs/C	113.31
Ru NPs/C	96.69
Pt/C (commercial)	82.47

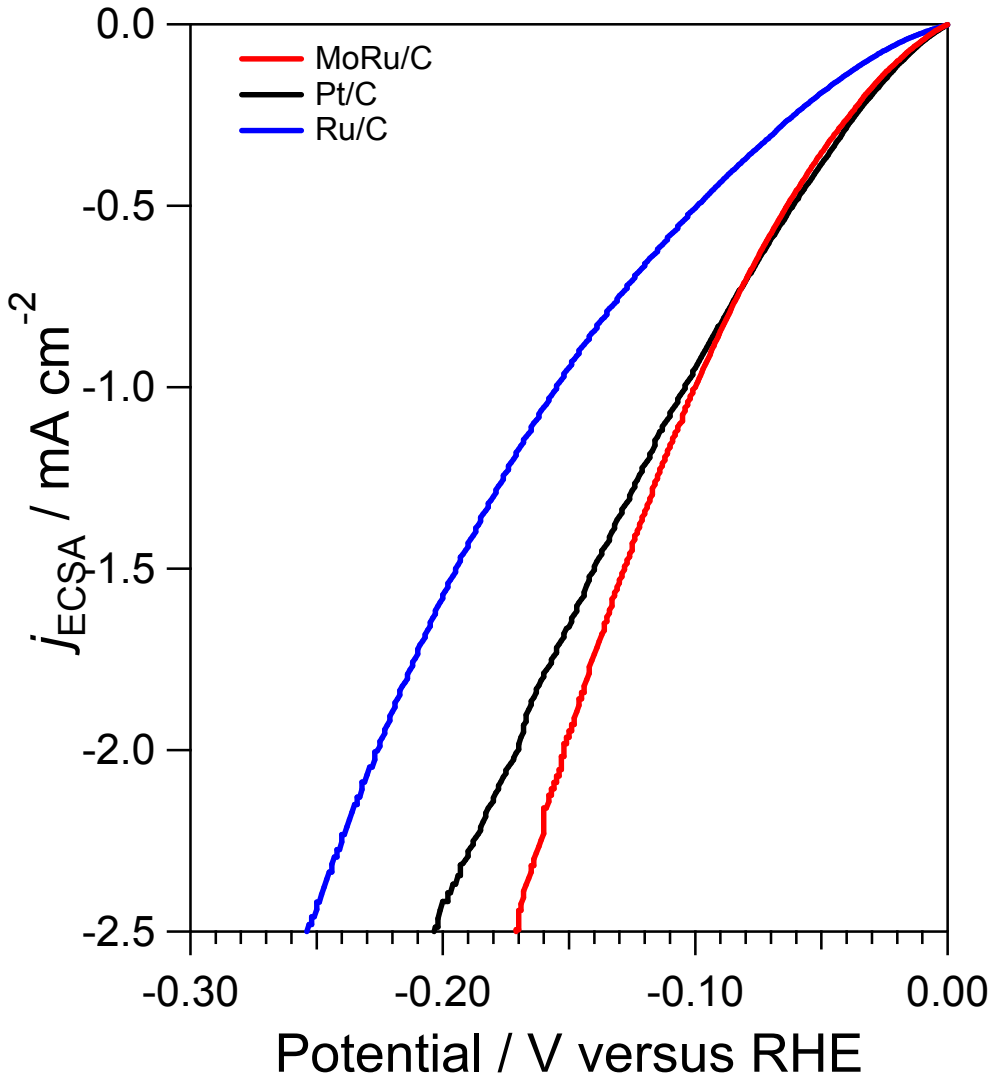

Fig. S20 Polarization curves of 20 wt% catalysts in 1.0 M KOH solution normalized by ECSA.

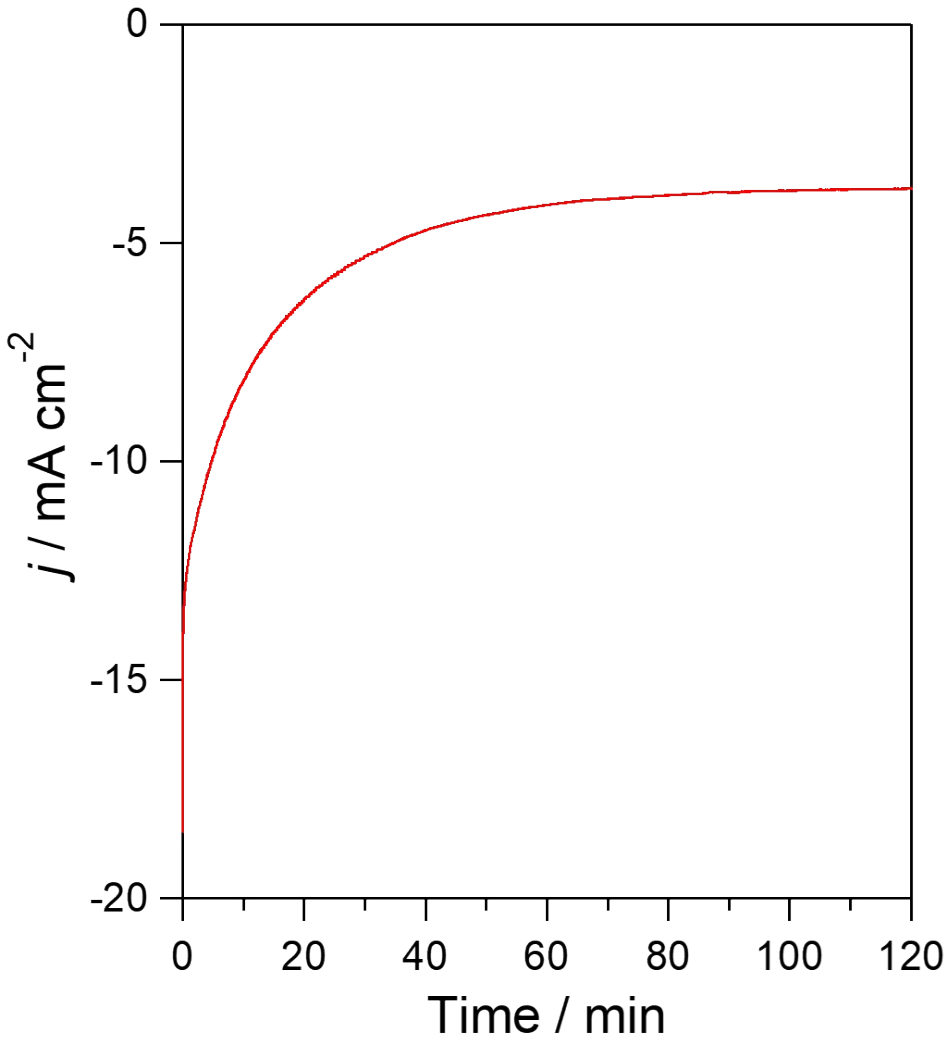

Fig. S21 Stability test of MoRu catalyst. The potential was maintained at the specific potential where geometry current density reached 10 mA cm^{-2} referring to HER result.

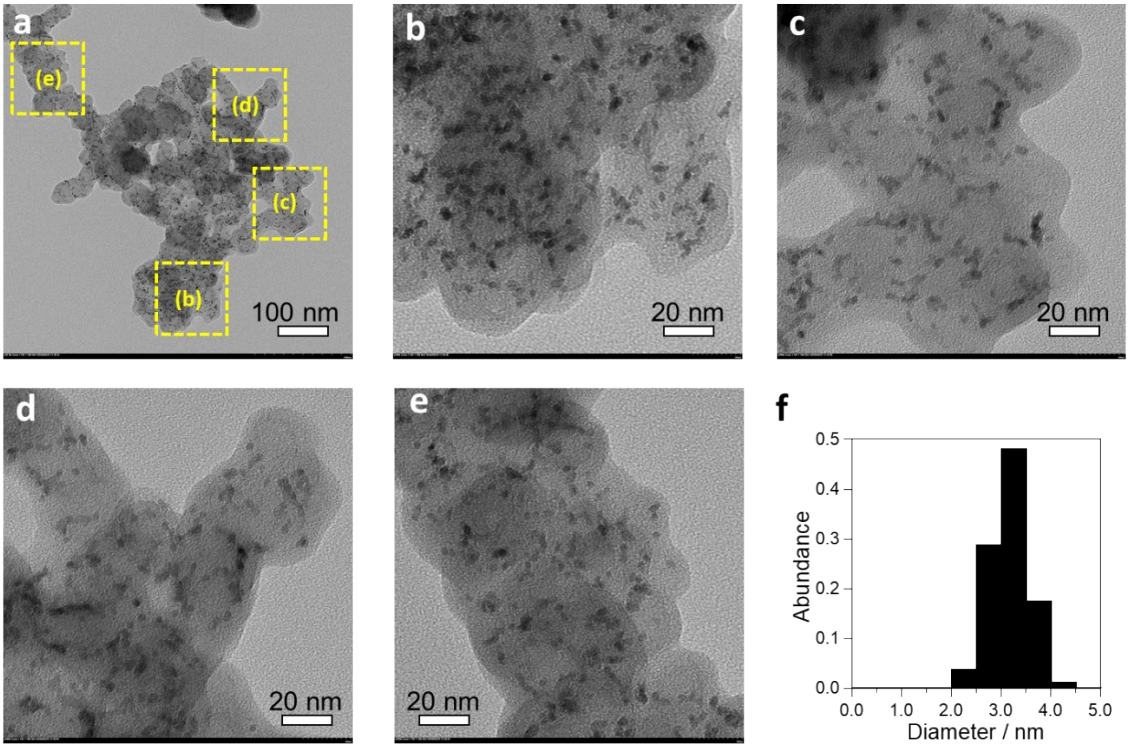

Fig. S22 TEM images MoRu/C after stability test. **a** Low magnification image. **b, c, d, e** Expanded images of **(a). f** Histogram of the size of NPs.

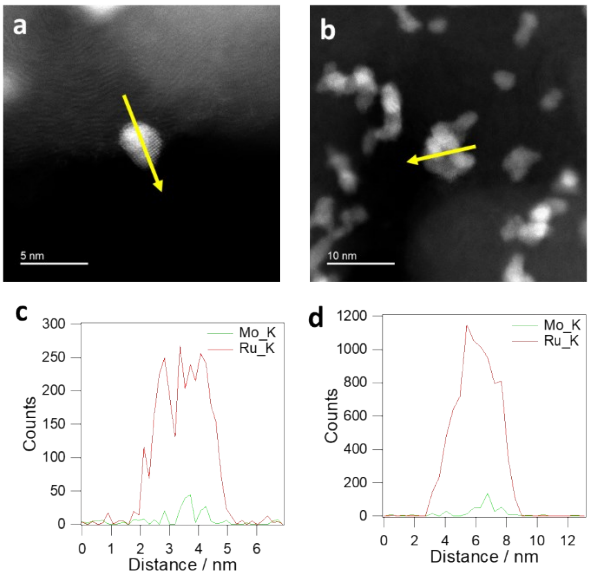

Fig. S23 EDX line profiles of the MoR/C after stability test. **a, b** HAADF-STEM image of MoRu NPs. **c, d** EDX line profiles of the MoRu NP along the arrow shown in **(a)**, **(b)** respectively. Mo and Ru are indicated as green and red lines, respectively. Due to the overlap of Mo-*L* and S-*K* line, these EDX line analyses were conducted with *K*-line.

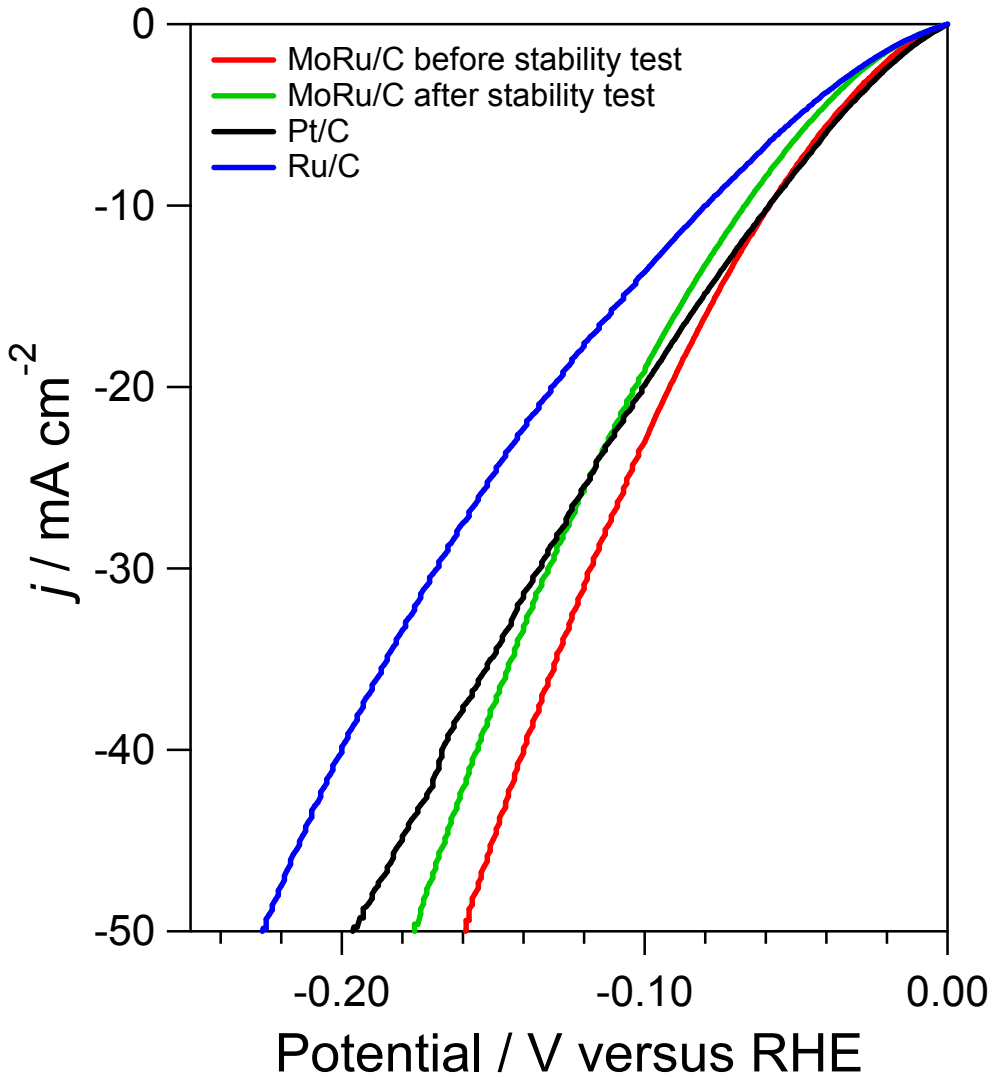

Fig. S24 Polarization curves of 20 wt% MoRu/C before and after stability test in 1.0 M KOH solution. Pt/C and Ru/C results are also shown for a comparison.

References

1. K. Kusada *et al.*, *J. Am. Chem. Soc.*, **2013**, *135*, 5493

2. C. Green and A. Kucernak, *J. Phys. Chem. B*, **2002**, *106*, 1036.